Effect of Nanoparticle Size on Thermal Performance of the Cylindrical Cavity Receiver

[1]Ph.D. graduated student, University of Mohaghegh Ardabili, Department of Biosystems Engineering, rloni@uma.ac.ir
[2]Facularity member, University of Tarbiat Modares, Department of Biosystems Engineering, ghobadib@modares.ac.ir
[3]Facularity member, University of Mohaghegh Ardabili, Department of Biosystems Engineering, ezzataskari@uma.ac.ir

ABSTRACT

In the current study, a dish concentrator using a cylindrical cavity receiver is considered. The Al_2O3/thermal oil is used as the solar working fluid. The main aim of this research is examined the effect of the nanoparticle size and nanofluid concentration on the thermal performance of the investigated solar system. The effect of nanoparticle size in the range of 0.5 nm to 50 nm, and nanofluid concentration in the range of 0% VF to 5% VF, are studied. The numerical thermal modeling is written by code in the Maple software, and the optical simulation is conducted in the SolTrace software. It is concluded that the thermal efficiency and heat gain of the cylindrical cavity receiver increases by decreasing the nanoparticle size and increasing nanofluid concentration. Also, it is conducted that the outlet temperature of the nanofluid decreases by increasing the nanoparticle size and increasing nanofluid concentration. The results of the current study shows that the appropriate condition for achieving the highest thermal performance of the cylindrical cavity receiver using alumina/thermal oil is including the smaller nanoparticle size and higher nanofluid concentration.

Keywords: Thermal performance; nanofluid concentration; nanoparticle size, cylindrical cavity receiver.

1- Introduction

Today, the attention to the dish concentrator as a compact and efficiently technology for producing thermal and power, is increased (Loni, Kasaeian, Asli-Ardeh, & Ghobadian, 2016; Loni, Kasaeian, Asli-Ardeh, Ghobadian, & Le Roux, 2016). Dish collector concentrates all of the incoming solar radiation to its focal point, where the receiver is located. There are different types of receiver for dish concentrator such as external receiver, spiral receiver, volume receiver, and cavity receiver (Pavlovic, Bellos, & Loni, 2017). Generally, the cavity receivers due to their special structure for reducing the thermal heat losses, have the higher efficiency compare to other types of receivers (Günther, Shahbazfar, Fend, & Hamdan).

There are some researches are considered the cylindrical cavity receiver as the absorber of the dish concentrators. Daabo et al. (Daabo, Mahmoud, & Al-Dadah, 2016) numerical evaluated the thermal and optical manner of a parabolic dish concentrator using three different shapes of cavity such as cylindrical, conical and spherical cavity receiver. Their results indicated that the conical cavity receiver has the highest optical and thermal performance. Loni et al. (Loni, Kasaeian, Asli-Ardeh, & Ghobadian, 2016) numerically considered the optimum structure of a cylindrical cavity receiver as the heat source of the ORC system. The thermal oil was applied as the solar heat transfer fluid. They investigated different parameters such as cavity depth, aperture diameter, inner tube diameter, mass flow rate, inlet temperature. Finally, the results reveal the optimum structure and operational parameters of the investigated cavity receiver. Xiao et al. (L. Xiao, Wu, & Li, 2012) theoretically evaluated the mixed convection heat losses from a cylindrical cavity receiver. Shen et al. (Shen, Wu, & Xiao, 2016) the mixed convection heat loss from a cylindrical cavity receiver under the windy conditions. The influence of different parameters such as the surface temperature, cavity tilt angle, wind incident angle, and wind speed were investigated.

Prakash et al. (Prakash, Kedare, & Nayak, 2009) researched a cylindrical cavity receiver numerically and experimentally. They considered the impacts of the working fluid inlet temperature, wind speed, and cavity inclination angle. They presented a Nusselt number for convection heat losses from the investigated cylindrical cavity receiver. Azzouzi et a. (Azzouzi, Boumeddane, & Abene, 2017) experimentally and numerically evaluated the thermal performance of a dish collector using a cylindrical cavity receiver and the water as the solar working fluid. They received a good agreement between their experimental results and their calculated

numerical study. Madadi et al. (Madadi, Tavakoli, & Rahimi, 2014) numerically and experimentally considered the energy and exergy efficiency of a dish collector using different cavity receivers such as cylindrical and conical cavity receiver. Water was used as the solar working fluid. They concluded that energy and exergy performance of the cylindrical cavity receiver was higher than the investigated conical cavity receiver. Wu et al. (Wu, Shen, Xiao, & Li, 2015) experimentally investigated a cylindrical cavity receiver under mixed convection heat losses. They presented the Nusselt number of the mixed convection heat losses under variation different parameters such as the wind speed, incident angle of the wind, and inclination angle of the cavity receiver.

Also, Wu et al. (Wu, Shen, & Xiao, 2015) experimentally considered a cylindrical cavity receiver under variation of cavity inclination, aperture ratio, and heat flux. The results indicated that the investigated parameters have a significant effect on the convection heat losses. Ma (Ma, 1993) conducted an experimental study for investigation of the forced convection heat losses of a cylindrical cavity receiver under the windy conditions. Mawire and Taole (Mawire & Taole, 2014) experimentally considered the energy and exergy performance of a new design of a dish collector using a cylindrical cavity receiver. Their investigated concentrator consists of heliostat reflecting mirrors that tracking the sun through a day. Then the reflected solar radiation is input in a parabolic dish concentrator. Finally, the total reflected solar radiation absorbed by the cylindrical cavity receiver that setup at the focal point of the dish collector. In their proposed design of the solar system, the dish collector is stable and the heliostat reflecting mirrors tracking the sun light. They studied the heat loss factor and optical efficiency of the considered setup. Xiao et al. (G. Xiao et al., 2014) experimentally evaluated a two-steps dish concentrator using a cylindrical cavity receiver for rotating a micro gas turbine and the air as the solar working fluid.

On the other hand, the attention on application of the nanofluid as the solar working fluid, is increased (). The thermal properties of the pure fluid can be improved by adding some nanoparticle to their. The combination of the pure fluid such as water and oil with the nanoparticles, calls “nanofluid”. Khullar et al. (Khullar et al., 2012) numerically investigated a nanofluid-based concentrating parabolic solar collector (NCPSC). The Al_2O_3/ Therminol VP-1 was used as the solar working fluid. The results show thermal performance enhancement about 5–10% for the investigate NCPSC compare to the conventional parabolic solar collector. Mahian et al. (Mahian, Kianifar, Sahin, & Wongwises, 2014b) numerically evaluated the first and second thermodynamic laws on the different water-based nanofluids (Cu/water, Al_2O_3/water, TiO_2/water, and SiO_2/water) in a minichannel-based solar collector. The results show the Cu/water nanofluid is the appropriate nanofluid for application in the investigated solar collector due to the highest outlet temperature and the lowest entropy generation.

Mahian et al. (Mahian, Kianifar, Sahin, & Wongwises, 2014a) numerically studied a flat plate collector using Al_2O_3/waste nanofluid as the solar working fluid. The influence of the four different nanoparticle sizes and different volume concentration was investigated on the heat transfer parameter of their investigated solar system. They concluded that the nanoparticle volume fraction has a direct relation with outlet temperature of the nanofluids. Mahian et al. (Mahian, Kianifar, Sahin, & Wongwises, 2015) analytically investigated the effect of the SiO_2/water nanofluid as the solar heat transfer fluid of a flat plate solar collector. The influence of the different values of pH and sizes of nanoparticles on the heat transfer, pressure drop, and entropy generation was evaluated during their study. They resulted that the outlet temperature increased and entropy generation decreased by the application of the nanofluid as the solar working fluid. Loni et al. (Loni, Asli-ardeh, Ghobadian, Kasaeian, & Gorjian, 2017) thermodynamically modeled a cavity receiver using different types of nanofluids. They resulted that Cu/thermal oil nanofluid had the best thermodynamic result on the investigated solar system. Mohammad Zadeh et al. (Zadeh, Sokhansefat, Kasaeian, Kowsary, & Akbarzadeh, 2015) numerically investigated the influence of the Al_2O_3/synthetic oil nanofluid as the solar working fluid of a parabolic trough collector. A hybrid optimization method was used as the optimization method for the investigated system. The results show that the higher nanoparticles concentration and lower operational temperature caused the higher heat transfer manner of the investigated solar system.

It can be seen from the aforementioned literature review that there is not any report of investigation of the nanoparticle size as the solar working in the dish concentrators. So, in the current study, the size and the volume fraction of the alumina nanoparticles in a cylindrical cavity receiver, is examined as a novelty idea. Thermal oil is used as the based fluid. The effect of nanoparticle size in the range of 0.5 nm to 50 nm, and nanofluid concentration in the range of 0% VF to 5% VF, are studied. The results of the current study is useful for

selection of the appropriate size and volume fraction of the alumina nanoparticles in the thermal oil for achieving the highest thermal efficiency.

2- Simulation and Methodology

A cylindrical cavity receiver is investigated in this study. A schematic of the cylindrical cavity receiver is shown in **Figure 1**. According to Le Roux et al. (Le Roux, Bello-Ochende, & Meyer, 2014), the factors contributing to the temperature profile and heat flow on the receiver wall can be divided into two components: geometry-dependent and temperature-dependent. Their research has shown that the effects of the geometry-dependent factors can be found with SolTrace software as an optical analysis software. The temperature-dependent factors including the radiation heat loss to the environment, the convection heat loss, and the conduction heat loss can be calculated from heat loss equations. In this study, these methods were applied to calculate the temperature profile and the heat flow on the receiver walls. The dimension of the investigated cylindrical cavity receiver is shown in Fig. 1.

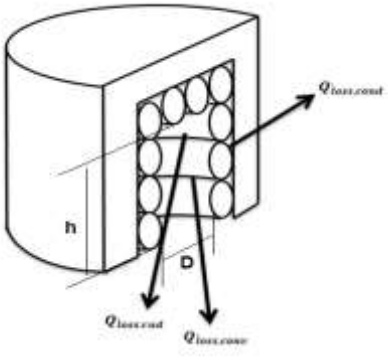

Figure 1: A schematic of the investigated cylindrical cavity receiver.

Table 1- The specification of the cavity receiver.

Parameters	Cylindrical Cavity Receiver
Outer diameter of the cavity aperture (D_{out})	16 cm
Inner diameter of cavity aperture (D_{in})	14 cm
Height of the cavity receiver (h)	14 cm
Number of tube turns at the cavity height	14
Diameter of the cavity inner tube (d_{tube})	10 (mm)
Insulation thickness (t_{ins})	2 (cm)
Average insulation conductivity (K_{ins})	0.062 (W/m.K)
Optical efficiency	0.93
Emissivity of the black chromium coating (ε)	0.01

The temperature-dependent factors could be calculated via the heat loss equations. These heat losses include the radiation heat loss to the environment, the convection heat loss, and the conduction heat loss. For preventing the heat loss, mineral wool was used as the receiver insulation. It should be mentioned that the overall heat losses due to conduction, radiation, and convection were calculated by assuming an average receiver surface temperature of 200°C. The net heat transfer rate ($\dot{Q}_{net}$) at the receiver tube is expressed as:

$$\dot{Q}_{net} = \dot{Q}^{*} - \dot{Q}_{loss,cond} - \dot{Q}_{loss,rad} - \dot{Q}_{loss,conv} \quad (1)$$

$$\dot{Q}^{*} = \eta_{optical}\eta_{refl}\dot{Q}_{solar} \quad (2)$$

$$\dot{Q}_{solar} = I_{sun}\pi D_{conc}^{2}/4 \quad (3)$$

where $\dot{Q}^{*}$ (W) is defined as the received solar heat flux to the cavity receiver, $\eta_{optical}$ is the optical efficiency, η_{refl} is the dish reflectivity efficiency, which is assumed equal to 0.84 in this analysis, $\dot{Q}_{solar}$ (W) is the total received solar heat flux by the dish concentrator, I_{sun} is the beam solar radiation (W/m^2), D_{conc} is the aperture dish diameter equal to 2 m. Also, $\dot{Q}_{loss,\ cond}$(W), $\dot{Q}_{loss,\ rad}$ (W) and $\dot{Q}_{loss,conv}$ (W) are the conduction heat loss, radiation heat loss, and convection heat loss, respectively, which are calculated in the next subsections. On the other side, the optical efficiency is defined as the ratio of the heat power absorbed by the cavity ($\dot{Q}_{ab}$) to the total received solar heat flux by the dish concentrator:

$$\eta_{optical} = \frac{\dot{Q}_{ab}}{\dot{Q}_{solar}} \quad (4)$$

It is worthy to notify that the $\dot{Q}_{ab}$ (W) was calculated by the SolTrace software. While the receiver thermal efficiency (η_{REC}) is defined as the ratio of the net heat transfer rate to the incoming solar beam radiation of the cavity receiver:

$$\eta_{th} = \dot{Q}_{net} / (\eta_{refl}\dot{Q}_{solar}) \quad (5)$$

The surface temperature ($T_{s,n}$) and the heat flow ($\dot{Q}_{net,n}$) at different elements of the tube are determined by solving Eqs. **(6)** and **(11)** using the Newton–Raphson Method [50]:

$$\dot{Q}_{net,n} = \frac{\left(T_{s,n} - \sum_{i=1}^{n-1}\left(\frac{\dot{Q}_{net,i}}{\dot{m}_{nf}c_{p,nf}}\right) - T_{inlet,0}\right)}{\left(\frac{1}{k_{inner}A_n} + \frac{1}{2\dot{m}_{nf}c_{p,nf}}\right)} \quad (6)$$

where, The heat transfer coefficient for the examined case is calculated according to Eq. **(7)** :

$$Nu_{inner} = \frac{\left(\frac{f_r}{8}\right).Re.Pr}{1 + 12.8.\sqrt{\frac{f_r}{8}}.(Pr^{0.68} - 1)} \quad (7)$$

The friction factor (f_r) has to be determined by the Eq. **(8)** as following:

$$f_r = (0.79\ln Re - 1.64)^{-2} \quad (8)$$

Moreover, the heat transfer coefficient is calculated as:

$$k_{inner} = \frac{Nu_{inner}K_{fluid}}{d_{tube}} \quad (9)$$

On the other hand, the net heat gained can be calculated with Eqs. **(6)** and **(11)** :

$$\dot{Q}_{net,n} = \dot{Q}^{*}_{n} - \dot{Q}_{loss,rad,n} - \dot{Q}_{loss,internal\ conv,n} - \dot{Q}_{loss,external\ conv,n} \quad (10)$$

$$\dot{Q}_{net,n} = \dot{Q}^{*}_{n} - A_n\varepsilon_n\sigma\left(T_{s,n}{}^4\right) + A_n\sum_{j=1}^{N}F_{n-j}\varepsilon_j\sigma\left(T_{s,n}{}^4\right) - A_n\varepsilon_n\sigma F_{n-\infty}T_{\infty}^4 - A_n\left(m_2T_{s,n} + c_2\right) - \frac{A_n}{R_{cond}}(T_{s,n} - T_{\infty}) \quad (11)$$

The receiver surface temperature at different elements of the tube and the heat flow depend on the receiver aperture size, the mass flow rate of the solar working fluid, the receiver tube diameter, and the working fluid inlet temperature. The optical parameters including the dish reflectivity, DNI (direct solar radiation) and the reflector surface optical error are the other parameters which effect on the thermal efficiency of the system. Each round of the spiral cavity receiver was assumed as a receiver element. The analysis is performed based on real meteorological data for three investigated cavity receivers for 11:00 AM in a typical day in Tehran, Iran (**Table 2**).

Table 2: Values of solar irradiance on the collector, ambient temperature, and wind velocity for 11:00 AM in a typical day (16 October 2016) in Tehran, Iran.

Wind speed (m/s)	1.5
Solar irradiation (W/m^2)	711
Ambient temperature (°C)	20.2

In this paper, the operation with nanofluids is investigated. Al_2O_3/thermal oil nanofluid is tested and its thermal properties are calculated according to the equations of this section. **Table 3** includes the thermal properties of the examined nanoparticle. It is obvious, that the nanoparticle present high density, high thermal conductivity and low specific heat capacity.

Table 3: Properties of nanoparticle.

Property	**Al_2O_3**
Thermal conductivity (W/m K)	40
Heat capacity (J/kg K)	765
Density (kg/m^3)	3970

Equations 30-33 give the thermal properties of the nanofluids. The base fluid is symbolized with (bf), the nanoparticle with (np) and the nanofluid with (nf).
The thermal conductivity of the nanofluid is calculated according to the suggested equation by Yu and Choi [45]:

$$k_{nf} = k_{bf} \cdot \frac{k_{np} + 2 \cdot k_{bf} + 2 \cdot (k_{np} - k_{bf}) \cdot (1+\beta)^3 \cdot \phi}{k_{np} + 2 \cdot k_{bf} - (k_{np} - k_{bf}) \cdot (1+\beta)^3 \cdot \phi} \quad (12)$$

The parameter β in this equation is the ratio of nano-layer thickness to the nanoparticles diameter which is considered to be 0.1 in of this study [46]. The density of the mixture is given by equation 2 [47] and the specific heat capacity according to equation 3 [48]:

$$\rho_{nf} = \rho_{bf} \cdot (1-\phi) + \rho_{np} \cdot \phi \quad (13)$$

$$c_{p,nf} = \frac{\rho_{bf} \cdot (1-\phi)}{\rho_{nf}} \cdot c_{p,bf} + \frac{\rho_{np} \cdot \phi}{\rho_{nf}} \cdot c_{p,np} \quad (14)$$

The dynamic viscosity is calculated according to the Batchelor model [49]:

$$\mu_{nf} = \mu_{bf} \cdot (1 + 2.5 \cdot \phi + 6.5 \cdot \phi^2) \quad (15)$$

3- Results and Discussion

Figure 3 shows the variation of thermal efficiency of the investigated cylindrical cavity receiver versus the variation of nanoparticle size at nanofluid concentration of 3% VF, and volume flow rate of 100 ml/s. It can be seen from **Figure 3**, the thermal efficiency of the cylindrical cavity receiver decreases by increasing the nanoparticle size. This issue is due to the decreasing cavity heat gain by increasing the nanoparticle size (see **Figure 3**). Consequently, it could be resulted that the thermal performance of the cylindrical cavity receiver is improved by application of smaller size of nanoparticle in the alumina/thermal oil nanofluid.

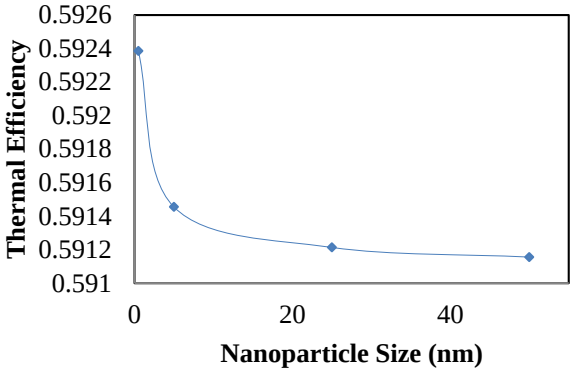

Figure 2: Variation of thermal efficiency versus the variation of nanoparticle size.

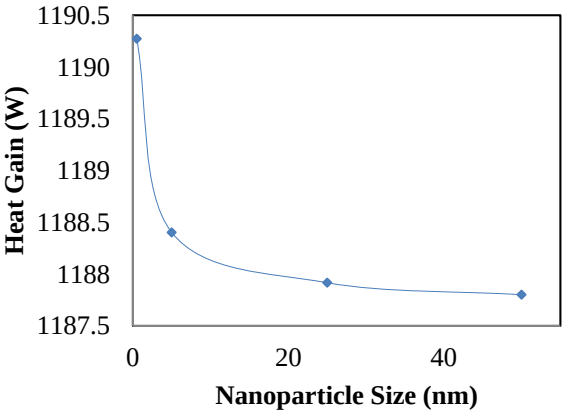

Figure 3: Variation of cavity heat gain versus the variation of nanoparticle size.

On the other side, the variation of outlet temperature of working fluid versus the variation of nanoparticle size is displayed at nanofluid concentration of 3% VF, and volume flow rate of 100 ml/s, in **Figure 4**. It could be seen that the outlet temperature of the investigated nanofluid has the same trend compare to the thermal efficiency, versus the nanoparticle size. In the other word, the outlet temperature of the nanofluid decrease by increasing the nanoparticle size. This issue is due to the decreasing cavity heat gain by increasing the nanoparticle size (see **Figure 3**). Consequently, the smaller nanoparticle size should be used for achieving the highest outlet temperature of the alumina/thermal oil as the solar working fluid in the cylindrical cavity receiver.

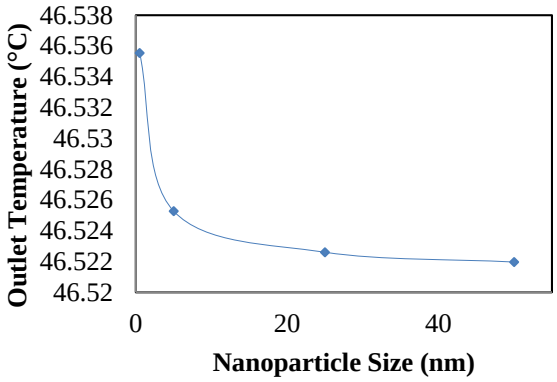

Figure 4: Variation of outlet temperature of working fluid versus the variation of nanoparticle size.

In this section the effect of the effect of the nanofluid concentration on the thermal performance of the cylindrical cavity receiver, is presented. The nanofluid concentration varies from 0.01 VF to 0.05 VF, whereas the nanofluid concentration of 0 VF, presented the pure thermal oil as the solar working fluid. **Figure 5** shows the variation of thermal efficiency of the cylindrical cavity receiver versus the variation of volume fraction of nanoparticle at nanoparticle size of 2 nm, and volume flow rate of 100 ml/s. As seen, the thermal efficiency of the cavity receiver improves by increasing the nanofluid concentration. This issue is due to the increasing the cavity heat gain by increasing the nanofluid concentration as shown in **Figure 6**. So, it could be resulted, the higher nanofluid concentration should be applied for achieving the higher thermal performance of the cylindrical cavity receiver using the alumina/thermal oil nanofluid.

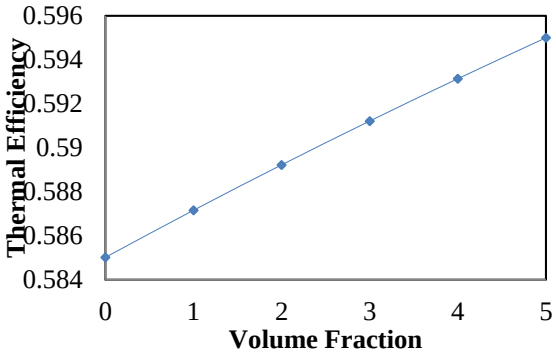

Figure 5: Variation of thermal efficiency versus the variation of volume fraction of nanoparticle.

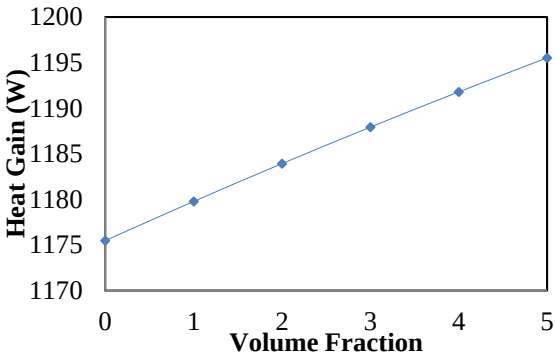

Figure 6: Variation of cavity heat gain versus the variation of volume fraction of nanoparticle.

Finally, the variation of outlet temperature of working fluid versus the variation of volume fraction of nanoparticle at nanoparticle size of 2 nm, and volume flow rate of 100 ml/s, is depicted in **Figure 7**. As displayed, the outlet temperature of the nanofluid decrease by increasing the nanofluid concentration of the alumina/thermal oil nanofluid. Consequently, the lower nanofluid concentration should be used for achieving the highest outlet temperature of the alumina/thermal oil as the solar working fluid in the cylindrical cavity receiver.

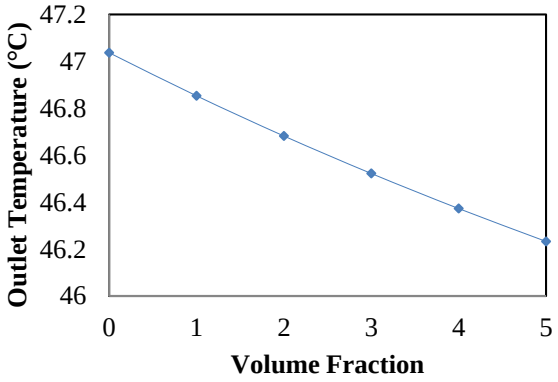

Figure 7: Variation of outlet temperature of working fluid versus the variation of volume fraction of nanoparticle.

4- Conclusion

In the current study, a dish concentrator using a cylindrical cavity receiver is studied. Alumina/thermal oil is used as the solar working fluid. The influence of the nanoparticle size and nanofluid concentration on the thermal performance of the investigated solar system, is considered. The main achievement could be summarized as following:

- The thermal efficiency, and heat gain of the cylindrical cavity receiver decreases by increasing the nanoparticle size.
- The outlet temperature of the nanofluid decrease by increasing the nanoparticle size. Consequently, the smaller nanoparticle size should be used for achieving the highest outlet temperature of the alumina/thermal oil as the solar working fluid in the cylindrical cavity receiver.
- The thermal efficiency, and heat gain of the cavity receiver improves by increasing the nanofluid concentration.
- The outlet temperature of the nanofluid decrease by increasing the nanofluid concentration of the alumina/thermal oil nanofluid. Consequently, the lower nanofluid concentration should be used for achieving the highest outlet temperature of the alumina/thermal oil as the solar working fluid in the cylindrical cavity receiver.

References

Azzouzi, D., Boumeddane, B., & Abene, A. (2017). Experimental and analytical thermal analysis of cylindrical cavity receiver for solar dish. *Renewable Energy*.

Daabo, A. M., Mahmoud, S., & Al-Dadah, R. K. (2016). The optical efficiency of three different geometries of a small scale cavity receiver for concentrated solar applications. *Applied Energy*, *179*, 1081-1096.

Günther, M., Shahbazfar, R., Fend, T., & Hamdan, M. Solar Dish Technology.

Khullar, V., Tyagi, H., Phelan, P. E., Otanicar, T. P., Singh, H., & Taylor, R. A. (2012). Solar energy harvesting using nanofluids-based concentrating solar collector. *Journal of Nanotechnology in Engineering and Medicine*, *3*(3), 031003.

Le Roux, W. G., Bello-Ochende, T., & Meyer, J. P. (2014). The efficiency of an open-cavity tubular solar receiver for a small-scale solar thermal Brayton cycle. *Energy Conversion and Management*, *84*, 457-470.

Loni, R., Asli-ardeh, E. A., Ghobadian, B., Kasaeian, A., & Gorjian, S. (2017). Thermodynamic analysis of a solar dish receiver using different nanofluids. *Energy*, *133*, 749-760.

Loni, R., Kasaeian, A., Asli-Ardeh, E. A., & Ghobadian, B. (2016). Optimizing the efficiency of a solar receiver with tubular cylindrical cavity for a solar-powered organic Rankine cycle. *Energy*, *112*, 1259-1272.

Loni, R., Kasaeian, A., Asli-Ardeh, E. A., Ghobadian, B., & Le Roux, W. (2016). Performance study of a solar-assisted organic Rankine cycle using a dish-mounted rectangular-cavity tubular solar receiver. *Applied thermal engineering*, *108*, 1298-1309.

Ma, R. Y. (1993). *Wind effects on convective heat loss from a cavity receiver for a parabolic concentrating solar collector*: Sandia National Laboratories.

Madadi, V., Tavakoli, T., & Rahimi, A. (2014). First and second thermodynamic law analyses applied to a solar dish

collector. *Journal of Non-Equilibrium Thermodynamics, 39*(4), 183-197.

Mahian, O., Kianifar, A., Sahin, A. Z., & Wongwises, S. (2014a). Entropy generation during Al_2O_3/water nanofluid flow in a solar collector: effects of tube roughness, nanoparticle size, and different thermophysical models. *International Journal of Heat and Mass Transfer, 78*, 64-75.

Mahian, O., Kianifar, A., Sahin, A. Z., & Wongwises, S. (2014b). Performance analysis of a minichannel-based solar collector using different nanofluids. *Energy Conversion and Management, 88*, 129-138.

Mahian, O., Kianifar, A., Sahin, A. Z., & Wongwises, S. (2015). Heat Transfer, Pressure Drop, and Entropy Generation in a Solar Collector Using SiO2/Water Nanofluids: Effects of Nanoparticle Size and pH. *Journal of Heat Transfer, 137*(6), 061011.

Mawire, A., & Taole, S. H. (2014). Experimental energy and exergy performance of a solar receiver for a domestic parabolic dish concentrator for teaching purposes. *Energy for sustainable development, 19*, 162-169.

Pavlovic, S., Bellos, E., & Loni, R. (2017). Exergetic investigation of a solar dish collector with smooth and corrugated spiral absorber operating with various nanofluids. *Journal of Cleaner Production*.

Prakash, M., Kedare, S., & Nayak, J. (2009). Investigations on heat losses from a solar cavity receiver. *Solar energy, 83*(2), 157-170.

Shen, Z.-G., Wu, S.-Y., & Xiao, L. (2016). Numerical study of wind effects on combined convective heat loss from an upward-facing cylindrical cavity. *Solar energy, 132*, 294-309.

Wu, S.-Y., Shen, Z.-G., & Xiao, L. (2015). Experimental investigation and uncertainty analysis on combined heat losses characteristics of a cylindrical cavity with only bottom wall heated at constant heat flux. *Heat Transfer Engineering, 36*(6), 539-552.

Wu, S.-Y., Shen, Z.-G., Xiao, L., & Li, D.-L. (2015). Experimental study on combined convective heat loss of a fully open cylindrical cavity under wind conditions. *International Journal of Heat and Mass Transfer, 83*, 509-521.

Xiao, G., Yan, L., Ni, M., Wang, C., Luo, Z., & Cen, K. (2014). Experimental Study of an Air Tube-cavity Solar Receiver. *Energy Procedia, 61*, 496-499.

Xiao, L., Wu, S.-Y., & Li, Y.-R. (2012). Numerical study on combined free-forced convection heat loss of solar cavity receiver under wind environments. *International journal of thermal sciences, 60*, 182-194.

Zadeh, P. M., Sokhansefat, T., Kasaeian, A., Kowsary, F., & Akbarzadeh, A. (2015). Hybrid optimization algorithm for thermal analysis in a solar parabolic trough collector based on nanofluid. *Energy, 82*, 857-864.